Published in final edited form as:
Nucl Med Biol. 2014 ; 41(10): 871–875. doi:10.1016/j.nucmedbio.2014.07.004.

Radiation Dosimetry and Biodistribution of the Translocator Protein Radiotracer [^{11}C]DAA1106 Determined with PET/CT in Healthy Human Volunteers

Arthur L. Brody, M.D.[1,2], **Kyoji Okita, M.D., Ph.D**[1,3], **Jennifer Shieh, B.S.**[1], **Lidia Liang, B.S.**[1], **Robert Hubert, B.A.**[1], **Michael Mamoun, M.D.**[1], **Judah Farahi, Ph.D.**[4], and **Mark A. Mandelkern, M.D., Ph.D.**[4,5]

[1]Department of Research, VA Greater Los Angeles Healthcare System (VAGLAHS), 11301 Wilshire Blvd., Los Angeles, CA 90073

[2]Department of Psychiatry, University of California at Los Angeles, 300 UCLA Medical Plaza, Suite 2200, Los Angeles, CA 90095

[3]UCLA Laboratory of Molecular Imaging, 760 Westwood Plaza C8-538, Los Angeles, CA 90095

[4]Department of Imaging, VAGLAHS, 11301 Wilshire Blvd., Los Angeles, CA 90073

[5]Department of Physics, University of California at Irvine, 4129 Frederick Reines Hall, Irvine, CA 92697

Abstract

Introduction—When microglia become activated (an integral part of neuroinflammation), cellular morphology changes and expression of translocator protein (TSPO) 18 kDa is increased. Over the past several years, [^{11}C]DAA1106 has emerged as a reliable radiotracer for labeling TSPO with high affinity during positron emission tomography (PET) scanning. While [^{11}C]DAA1106 PET scanning has been used in several research studies, a radiation dosimetry study of this radiotracer in humans has not yet been published.

Methods—Twelve healthy participants underwent full body dynamic [^{11}C]DAA1106 PET scanning, with 8 sequential whole body scans (approximately 12 bed positions each), following a single injection. Regions of interest were drawn manually and time activity curves (TACs) were obtained for 15 organs. OLINDA/EXM 1.1 was used to compute radiation absorbed doses to the target organs, as well as effective dose (ED) and effective dose equivalent (EDE).

Results—The ED and EDE were 4.06 ± 0.58 μSv/MBq and 5.89 ± 0.83 μSv/MBq, respectively. The highest absorbed doses were to the heart wall, kidney, liver, pancreas, and spleen. TACs revealed that peak dose rates are during the first scan (at 6 min) for all organs other than the urinary bladder wall, which had its peak dose rate during the fourth scan (at 30 min).

Corresponding Author: Arthur L. Brody, M.D., 300 UCLA Medical Plaza, Suite 2200, Los Angeles, CA 90095, Phone: 310-268-4778; Fax: 310-206-2802, abrody@ucla.edu.

Conclusions—The recently developed radiotracer [^{11}C]DAA1106 has its EDE and target-organ absorbed dose such that, for a single administration, its radiation dosimetry is well within the U.S. FDA guidelines for basic research studies in adults. This dose level implies that the dosimetry for multiple [^{11}C]DAA1106 scans within a given year also falls within FDA guidelines, and this favorable property makes this radiotracer suitable for examining microglial activation repeatedly over time, which may in the future be useful for longitudinal tracking of disease progression and monitoring of therapy response in conditions marked by neuroinflammation (e.g., head trauma and multiple sclerosis).

Keywords

[^{11}C]DAA1106; positron emission tomography; dosimetry; neuroinflammation; translocator protein; review

Introduction

The change in microglia from the resting to the activated state is known to be an integral part of neuroinflammation [1]. Functions of activated microglia include: clearance of apoptotic cells and extracellular pathogens, removal of degenerating neurons and extracellular proteins, and cytokine/chemokine production. When microglia become activated, cellular morphology changes and expression of translocator protein (TSPO) 18 kDa is increased [1], thereby making expression of TSPO a marker for neuroinflammation.

Over the past several years, the radioligand N-(2,5-dimethoxybenzyl)-N-(5-fluoro- 2-phenoxyphenyl) acetamide labeled with carbon-11 (abbreviated as [^{11}C]DAA1106) has emerged as a reliable radiotracer for examining neuroinflammation with positron emission tomography (PET) scanning *in vivo* [2]. This radiotracer labels TSPO with high affinity, and this mitochondrial protein is found in brain and peripheral tissues [3]. Specific binding of DAA1106 has been found to correlate with the presence of activated microglia identified by immunohistochemistry *in situ*[4]. Furthermore, immunohistochemistry combined with autoradiography in brain tissues, as well as correlational analyses, show that increased DAA1106 binding in the central nervous system corresponds mainly to the presence of activated microglia [2, 5].

[^{11}C]DAA1106 was originally developed as a radiotracer for measuring inflammation [6–8], and was determined to have higher binding than previously used radiotracers [2, 4, 9, 10]. In animal studies using this radiotracer [10], binding was significant in cortex, brainstem, hippocampus, and cerebellum, and neural destruction was found to result in increased binding. In addition, specific binding was estimated to be 80% of total binding [10], which is a favorable property for a radiotracer.

PET scanning and [^{11}C]DAA1106 have been used in a growing number of studies to examine conditions thought to be associated with neuroinflammation. For example, this method was used recently to demonstrate widespread neuroinflammation in patients with mild cognitive impairment and Alzheimer's Disease (AD) compared to age-matched controls [11]. Similarly, a prior study found increased [^{11}C]DAA1106 binding in participants with AD compared with control subjects across many regions, including dorsal

and medial prefrontal cortex, lateral temporal cortex, parietal cortex, occipital cortex, anterior cingulate cortex, striatum, and cerebellum [12]. [(3)H]DAA1106 binding was also found to be elevated in a rat model of traumatic brain injury [13, 14]. Additionally, in a recent study, researchers found no significant difference between [^{11}C]DAA1106 binding in cortical regions of patients with schizophrenia compared to normal controls [15]. While [^{11}C]DAA1106 PET scanning has been used in these studies, a radiation dosimetry study of this radiotracer in humans has not yet been published. Therefore, we performed this dosimetry study of [^{11}C]DAA1106 to inform future research studies using this radiotracer.

Methods

Radiochemistry

[^{11}C]DAA1106 was synthesized by an established method [16, 17], in which the tracer was radiolabeled using [^{11}C]methyl iodide via a captive solvent method (Figure 1) [18]. No-carrier-added [^{11}C] CH_4 was produced using a TR-19 cyclotron by proton bombardment of 10% hydrogen in nitrogen gas. The radiochemical purity was >99%, with mean specific activity (± SD) of 17.6 ± 13.1 Ci/μmol.

Participants

Twelve healthy participants (ten men and two women; mean age 53 ± 14 y; age range 26 to 65 y) completed the study. Participants were veterans, and weighed 88 ± 17 kg (range 67 to 112 kg). Each participant provided written informed consent using a form approved by the local Institutional Review Board at a screening visit prior to PET scanning. Participants were generally healthy, based on their reports, a physical examination, and reviews of medical records, which included routine laboratory tests. Exclusion criteria consisted of conditions that might affect a participant's ability to tolerate study procedures, such as severe liver or kidney disease, current mental illness, or cardiovascular disease. Participants were also excluded if they were regularly taking anti-inflammatory medication or were pregnant. Breathalyzer and urine toxicology screens were obtained for all participants, and urine pregnancy tests were obtained for women of childbearing potential. Potential participants were excluded from undergoing PET scanning if any of these tests were positive.

PET/CT Acquisition and PET Image Analysis

Participants underwent full body dynamic [^{11}C]DAA1106 PET scanning obtained with the Philips Gemini TruFlight PET Scanner (Koninklijke Philips Electronics N.V., Eindhoven, the Netherlands). Following intravenous bolus injection of 369 ± 70 MBq [^{11}C]DAA1106 over 30 seconds, each participant had 8 sequential whole body scans (three 30-sec, three 1-min, and two-2 min at each bed position) with approximately 12 bed positions each (from the vertex to the mid-thigh). There was minimal acquisition delay between bed positions, while there was a 5–10 second delay between scans for the return movement of the bed. Each bed position had 50% overlap with the previous bed position (other than the first bed position). Mean scanning times were 6, 12, 18, 30, 42, 54, 78, and 102 minutes after injection. Participants were continuously scanned and did not urinate during the procedure. PET images were acquired in time-of-flight mode and reconstructed with the RAMLA

iterative algorithm [19]. Images were corrected for scatter and attenuation based on the CT scan.

Regions of interest (ROIs) were drawn manually on the images and time activity curves (TACs) were obtained for brain, gallbladder contents, small intestine, stomach wall, heart contents, heart wall, kidneys, liver, lungs, muscle, pancreas, red marrow, spleen, thyroid, and urinary bladder contents. The TACs were integrated to yield the number of disintegrations per mCi in each source organ. The total number of disintegrations per mCi in the body is given by $t_{1/2}/\ln 2 = 0.489$ hr. The numbers for the individual organs were scaled so that the total has this value. This step removed uncertainty in the activity that reached the circulation. OLINDA/EXM (Organ Level INternal Dose Assessment/EXponential Modeling) 1.1 [20] was used to compute radiation doses to the target organs as well as effective dose (ED) and effective dose equivalent (EDE), using the adult male (n = 10) and female (n = 2) models.

Results

Participants did not report any subjective effects following the injected dose of [^{11}C]DAA1106. No adverse events or serious adverse events occurred following radiotracer injection, and no significant changes in vital signs or clinical laboratory tests (CBC and chemistry panel) were found from before to after PET scanning.

The highest absorbed doses were to the heart wall, kidney, liver, pancreas, and spleen (Table 1). These organs were visible on participant PET scans (Figure 2). The total ED and EDE were 4.06 ± 0.58 μSv/MBq and 5.89 ± 0.83 μSv/MBq, respectively. Time activity curves (TACs) (Figure 3) revealed that peak dose rates are during the first scan (at 6 min) for all organs other than the urinary bladder wall, which had its peak dose rate during the fourth scan (at 30 min). The liver, lungs, and kidneys received the highest percentages of the injected dose.

The following is worth noting. OLINDA computes target-organ doses for a hypothetical uterus and hypothetical ovaries, even for the male model. If the equivalent dose to the “ovaries” exceeds that to the testes, the former is used in the EDE and ED calculations. If the “uterus” receives a sufficient equivalent dose, it is used in the EDE and/or ED calculations. For DAA in our male subjects, OLINDA uses “ovaries” in lieu of testes in the EDE and ED calculations and uses “uterus” in the ED calculation. If we modify the calculations so that, for the male subjects (n=10), testes is used for EDE and ED and “uterus” is not used, EDE (ED) is reduced by 14% (13%).

Discussion

The recently developed radiotracer [^{11}C]DAA1106 has an EDE of 5.89 ± 0.83 μSv/MBq and comparably small equivalent radiation doses to the critical organs (blood-forming organs and gonads). These findings mean that a PET scanning session with injection of a single injection of 370 MBq of [^{11}C]DAA1106 is well within the U.S. Food and Drug Administration guidelines (Code of Federal Regulation, Title 21, Part 361.1) for exposure to adults in a basic research study. This EDE value is also within the range of EDE values

(3.3–17.4 μSv/MBq) from a recent review of [^{11}C] radiotracer dosimetry studies [21]. The radiation doses found here are such that multiple scans with [^{11}C]DAA1106 within a given year also would fall within FDA guidelines for research. This favorable property of [^{11}C]DAA1106 makes it suitable for examining microglial activation (a marker for neuroinflammation) repeatedly over time, which could be useful for research into conditions that are marked by neuroinflammation (e.g., head trauma [22, 23] or multiple sclerosis [24, 25]) and where longitudinal tracking might be helpful.

Radiation dosimetry and biodistribution of [^{11}C]DAA1106 are also similar to other radiotracers that are used to label TSPO. The ED and EDE found here are slightly lower than those found for the TSPO radiotracers [^{11}C]PK11195 [26, 27] and [^{11}C]PBR28 [28]. In addition, the target organs with the highest doses from [^{11}C]DAA1106 (heart wall, kidneys, liver, pancreas, and spleen) are similar to the target organs most commonly found to have relatively high dose in other studies of TSPO radiotracers in humans [26–29] and laboratory animals [29, 30]. While it is somewhat unexpected that the heart wall would have a relatively high dose, this finding is consistent with prior research using radiotracers for TSPO, where this organ has a moderate-to-high [26, 27, 29, 30] dose, due to persistent activity in the myocardium. The consistency of this finding may indicate that specific binding in this organ contributes to the absorbed dose.

In addition to [^{11}C]DAA1106 having slightly lower ED and EDE values than most TSPO radiotracers, this radiotracer has other favorable properties. To our knowledge, the most commonly used TSPO radiotracer for examining neuroinflammation in a variety of conditions in humans is [^{11}C]PK11195 (e.g., [31–36]). Like [^{11}C]PK11195 and similar radiotracers, [^{11}C]DAA1106 is a potent and selective radioligand for TSPO (formerly called the peripheral benzodiazepine receptor) [6], with [^{11}C]DAA1106 having about 80% specific binding in brain [10]. In a study directly comparing DAA1106 with PK11195, DAA1106 was found to have a lower dissociation constant [2, 4] and higher specific binding at the site of an experimentally induced lesion than PK11195 [2], which led the study authors to conclude that DAA1106 may be a better radioligand for human PET studies than the commonly used PK11195. This last point has also been suggested as being advantageous for DAA1106 for visualizing TSPO levels in conditions characterized by mild neuroinflammation [37]. Thus, in addition to other similar radiotracers, [^{11}C]DAA1106 may prove useful for studying and monitoring disease progression and therapy response in conditions associated with neuroinflammation [38], such as head trauma [22, 23] and multiple sclerosis [24, 25].

Conclusion

The biodistribution and radiation dosimetry of [^{11}C]DAA1106 are similar to other [^{11}C] radiotracers used for PET scanning. Furthermore, the ED and EDE for [^{11}C]DAA1106 are slightly lower than those of other current radiotracers used to examine neuroinflammation, which is a favorable characteristic. These properties make [^{11}C]DAA1106 suitable for the examination of neuroinflammation in studies that use either single or multiple radiotracer injections.

Acknowledgments

This study was supported by the National Institute on Drug Abuse (A.L.B. [R01 DA20872]), the Tobacco-Related Disease Research Program (A.L.B. [19XT-0135]), and the Department of Veterans Affairs, Office of Research and Development (CSR&D Merit Review Award I01 CX000412 [A.L.B.]). The sponsors had no role in the design and conduct of the study; collection, management, analysis, and interpretation of the data; or preparation, review, or approval of the manuscript.

Bibliography

1. Anthony DC, Pitossi FJ. Special issue commentary: The changing face of inflammation in the brain. Mol Cell Neurosci. 2012
2. Venneti S, Lopresti BJ, Wang G, Slagel SL, Mason NS, Mathis CA, et al. A comparison of the high-affinity peripheral benzodiazepine receptor ligands DAA1106 and (R)-PK11195 in rat models of neuroinflammation: implications for PET imaging of microglial activation. J Neurochem. 2007; 102:2118–31. [PubMed: 17555551]
3. Rupprecht R, Papadopoulos V, Rammes G, Baghai TC, Fan J, Akula N, et al. Translocator protein (18 kDa) (TSPO) as a therapeutic target for neurological and psychiatric disorders. Nat Rev Drug Discov. 2010; 9:971–88. [PubMed: 21119734]
4. Venneti S, Wang G, Nguyen J, Wiley CA. The positron emission tomography ligand DAA1106 binds with high affinity to activated microglia in human neurological disorders. J Neuropathol Exp Neurol. 2008; 67:1001–10. [PubMed: 18800007]
5. Gulyas B, Makkai B, Kasa P, Gulya K, Bakota L, Varszegi S, et al. A comparative autoradiography study in post mortem whole hemisphere human brain slices taken from Alzheimer patients and age-matched controls using two radiolabelled DAA1106 analogues with high affinity to the peripheral benzodiazepine receptor (PBR) system. Neurochem Int. 2009; 54:28–36. [PubMed: 18984021]
6. Zhang MR, Kida T, Noguchi J, Furutsuka K, Maeda J, Suhara T, et al. [(11)C]DAA1106: radiosynthesis and in vivo binding to peripheral benzodiazepine receptors in mouse brain. Nucl Med Biol. 2003; 30:513–9. [PubMed: 12831989]
7. Chaki S, Funakoshi T, Yoshikawa R, Okuyama S, Okubo T, Nakazato A, et al. Binding characteristics of [3H]DAA1106, a novel and selective ligand for peripheral benzodiazepine receptors. Eur J Pharmacol. 1999; 371:197–204. [PubMed: 10357257]
8. Okubo T, Yoshikawa R, Chaki S, Okuyama S, Nakazato A. Design, synthesis and structure-affinity relationships of aryloxyanilide derivatives as novel peripheral benzodiazepine receptor ligands. Bioorg Med Chem. 2004; 12:423–38. [PubMed: 14723961]
9. Leung, K. N-(5-Fluoro-2-phenoxyphenyl)-N-(2-[18F]fluoroethyl-5-methoxybenzyl)acetamide. 2004.
10. Maeda J, Suhara T, Zhang MR, Okauchi T, Yasuno F, Ikoma Y, et al. Novel peripheral benzodiazepine receptor ligand [11C]DAA1106 for PET: an imaging tool for glial cells in the brain. Synapse. 2004; 52:283–91. [PubMed: 15103694]
11. Yasuno F, Kosaka J, Ota M, Higuchi M, Ito H, Fujimura Y, et al. Increased binding of peripheral benzodiazepine receptor in mild cognitive impairment-dementia converters measured by positron emission tomography with [(11)C]DAA1106. Psychiatry Res. 2012; 203:67–74. [PubMed: 22892349]
12. Yasuno F, Ota M, Kosaka J, Ito H, Higuchi M, Doronbekov TK, et al. Increased binding of peripheral benzodiazepine receptor in Alzheimer's disease measured by positron emission tomography with [11C]DAA1106. Biol Psychiatry. 2008; 64:835–41. [PubMed: 18514164]
13. Venneti S, Wagner AK, Wang G, Slagel SL, Chen X, Lopresti BJ, et al. The high affinity peripheral benzodiazepine receptor ligand DAA1106 binds specifically to microglia in a rat model of traumatic brain injury: implications for PET imaging. Exp Neurol. 2007; 207:118–27. [PubMed: 17658516]
14. Yu I, Inaji M, Maeda J, Okauchi T, Nariai T, Ohno K, et al. Glial cell-mediated deterioration and repair of the nervous system after traumatic brain injury in a rat model as assessed by positron emission tomography. J Neurotrauma. 2010; 27:1463–75.

15. Takano A, Arakawa R, Ito H, Tateno A, Takahashi H, Matsumoto R, et al. Peripheral benzodiazepine receptors in patients with chronic schizophrenia: a PET study with [11C]DAA1106. Int J Neuropsychopharmacol. 2010; 13:943–50. [PubMed: 20350336]
16. Wang M, Gao M, Zheng QH. Fully automated synthesis of PET TSPO radioligands [11C]DAA1106 and [18F]FEDAA1106. Appl Radiat Isot. 2012; 70:965–73. [PubMed: 22469868]
17. Probst KC, Izquierdo D, Bird JL, Brichard L, Franck D, Davies JR, et al. Strategy for improved [(11)C]DAA1106 radiosynthesis and in vivo peripheral benzodiazepine receptor imaging using microPET, evaluation of [(11)C]DAA1106. Nucl Med Biol. 2007; 34:439–46. [PubMed: 17499734]
18. Wilson AA, Garcia A, Jin L, Houle S. Radiotracer synthesis from [(11)C]-iodomethane: a remarkably simple captive solvent method. Nucl Med Biol. 2000; 27:529–32. [PubMed: 11056365]
19. Surti S, Kuhn A, Werner ME, Perkins AE, Kolthammer J, Karp JS. Performance of Philips Gemini TF PET/CT scanner with special consideration for its time-of-flight imaging capabilities. J Nucl Med. 2007; 48:471–80. [PubMed: 17332626]
20. Stabin MG, Sparks RB, Crowe E. OLINDA/EXM: the second-generation personal computer software for internal dose assessment in nuclear medicine. J Nucl Med. 2005; 46:1023–7. [PubMed: 15937315]
21. van der Aart J, Hallett WA, Rabiner EA, Passchier J, Comley RA. Radiation dose estimates for carbon-11-labelled PET tracers. Nucl Med Biol. 2012; 39:305–14. [PubMed: 22033023]
22. Finnie JW. Neuroinflammation: beneficial and detrimental effects after traumatic brain injury. Inflammopharmacology. 2013; 21:309–20. [PubMed: 23296919]
23. Smith C. Review: the long-term consequences of microglial activation following acute traumatic brain injury. Neuropathology and applied neurobiology. 2013; 39:35–44. [PubMed: 23206160]
24. Ellwardt E, Zipp F. Molecular mechanisms linking neuroinflammation and neurodegeneration in MS. Exp Neurol. 2014
25. Frank-Cannon TC, Alto LT, McAlpine FE, Tansey MG. Does neuroinflammation fan the flame in neurodegenerative diseases? Molecular neurodegeneration. 2009; 4:47. [PubMed: 19917131]
26. Hirvonen J, Roivainen A, Virta J, Helin S, Nagren K, Rinne JO. Human biodistribution and radiation dosimetry of 11C-(R)-PK11195, the prototypic PET ligand to image inflammation. European journal of nuclear medicine and molecular imaging. 2010; 37:606–12. [PubMed: 19862517]
27. Kumar A, Muzik O, Chugani D, Chakraborty P, Chugani HT. PET-derived biodistribution and dosimetry of the benzodiazepine receptor-binding radioligand (11)C-(R)-PK11195 in children and adults. J Nucl Med. 2010; 51:139–44. [PubMed: 20008990]
28. Brown AK, Fujita M, Fujimura Y, Liow JS, Stabin M, Ryu YH, et al. Radiation dosimetry and biodistribution in monkey and man of 11C-PBR28: a PET radioligand to image inflammation. J Nucl Med. 2007; 48:2072–9. [PubMed: 18006619]
29. Arlicot N, Vercouillie J, Ribeiro MJ, Tauber C, Venel Y, Baulieu JL, et al. Initial evaluation in healthy humans of [18F]DPA-714, a potential PET biomarker for neuroinflammation. Nucl Med Biol. 2012; 39:570–8. [PubMed: 22172392]
30. Verschuer JD, Towson J, Eberl S, Katsifis A, Henderson D, Lam P, et al. Radiation dosimetry of the translocator protein ligands [18F]PBR111 and [18F]PBR102. Nucl Med Biol. 2012; 39:742–53. [PubMed: 22300959]
31. Su Z, Herholz K, Gerhard A, Roncaroli F, Du Plessis D, Jackson A, et al. [(1)(1)C]-(R)PK11195 tracer kinetics in the brain of glioma patients and a comparison of two referencing approaches. European journal of nuclear medicine and molecular imaging. 2013; 40:1406–19. [PubMed: 23715902]
32. Varrone A, Mattsson P, Forsberg A, Takano A, Nag S, Gulyas B, et al. In vivo imaging of the 18-kDa translocator protein (TSPO) with [18F]FEDAA1106 and PET does not show increased binding in Alzheimer's disease patients. European journal of nuclear medicine and molecular imaging. 2013; 40:921–31. [PubMed: 23436070]

33. Suzuki K, Sugihara G, Ouchi Y, Nakamura K, Futatsubashi M, Takebayashi K, et al. Microglial activation in young adults with autism spectrum disorder. JAMA psychiatry. 2013; 70:49–58. [PubMed: 23404112]

34. Edison P, Ahmed I, Fan Z, Hinz R, Gelosa G, Ray Chaudhuri K, et al. Microglia, amyloid, and glucose metabolism in Parkinson's disease with and without dementia. Neuropsychopharmacology. 2013; 38:938–49. [PubMed: 23303049]

35. Iannaccone S, Cerami C, Alessio M, Garibotto V, Panzacchi A, Olivieri S, et al. In vivo microglia activation in very early dementia with Lewy bodies, comparison with Parkinson's disease. Parkinsonism & related disorders. 2013; 19:47–52. [PubMed: 22841687]

36. Schuitemaker A, Kropholler MA, Boellaard R, van der Flier WM, Kloet RW, van der Doef TF, et al. Microglial activation in Alzheimer's disease: an (R)-[(1)(1)C]PK11195 positron emission tomography study. Neurobiol Aging. 2013; 34:128–36. [PubMed: 22840559]

37. Doorduin J, Klein HC, de Jong JR, Dierckx RA, de Vries EF. Evaluation of [11C]-DAA1106 for imaging and quantification of neuroinflammation in a rat model of herpes encephalitis. Nucl Med Biol. 2010; 37:9–15. [PubMed: 20122662]

38. Doorduin J, de Vries EF, Dierckx RA, Klein HC. PET imaging of the peripheral benzodiazepine receptor: monitoring disease progression and therapy response in neurodegenerative disorders. Current pharmaceutical design. 2008; 14:3297–315. [PubMed: 19075709]

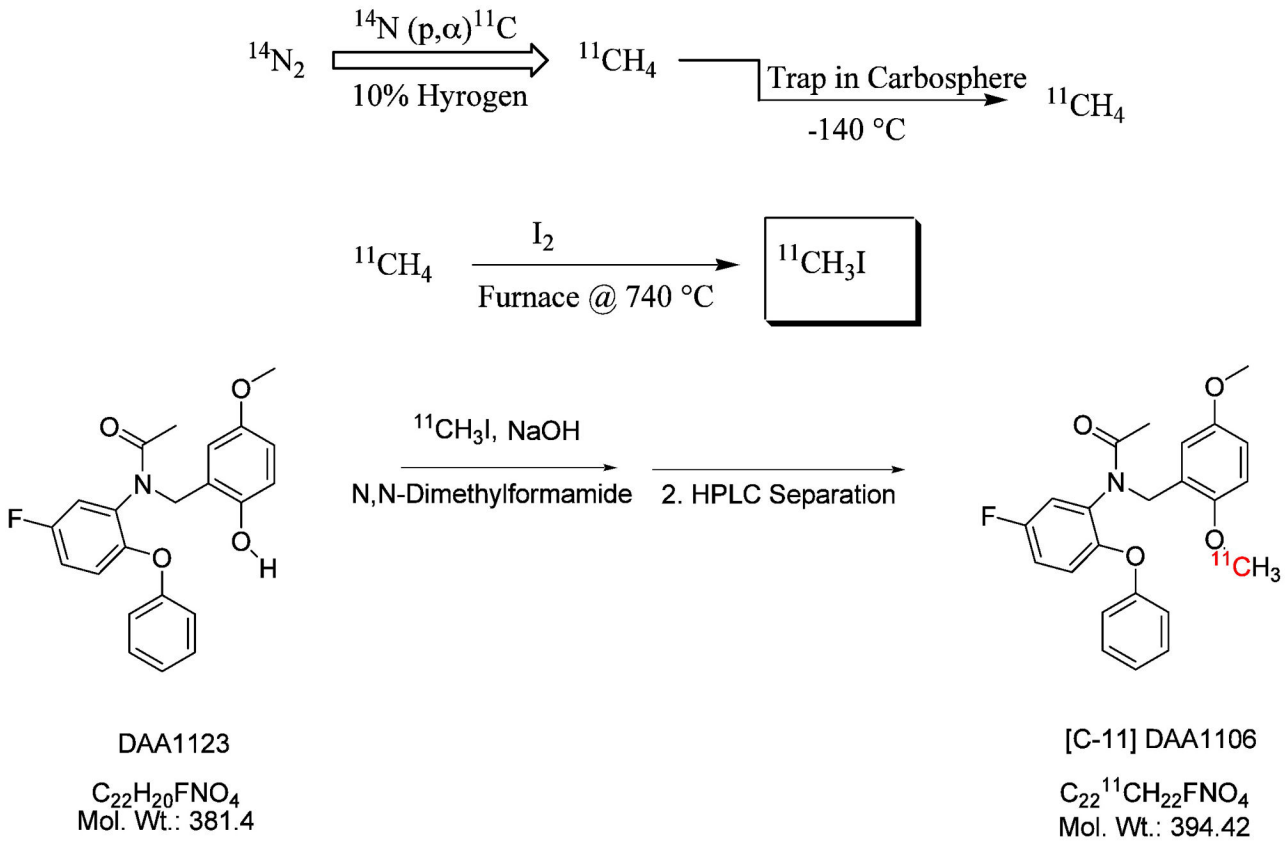

Figure 1.

[^{11}C]DAA1106 was synthesized in radiolabeled form from ^{11}C-methyl iodide via a captive-solvent method developed by Wilson et al., known as the loop method. No-carrier-added [^{11}C]CH_4 was produced in the TR-19 cyclotron by proton bombardment of 10% hydrogen in nitrogen gas.

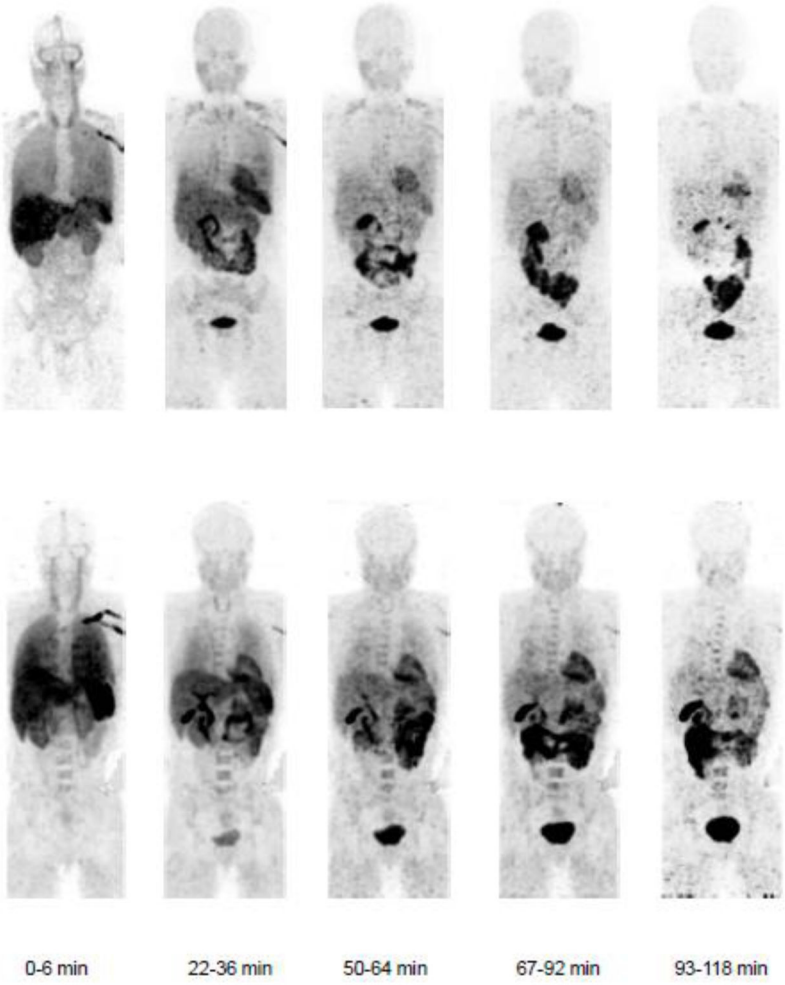

Figure 2.

Whole-body images of a healthy male (top) and a healthy female (bottom) participant showing biodistribution of [^{11}C]DAA1106 with imaging intervals of 0–6 minutes, 22–36 minutes, 50–64 minutes, 67–92 minutes, 93–118 minutes after injection of ~369 MBq [^{11}C]DAA1106. All coronal slices of the scan were summed, decay-corrected, and displayed using the same gray scale.

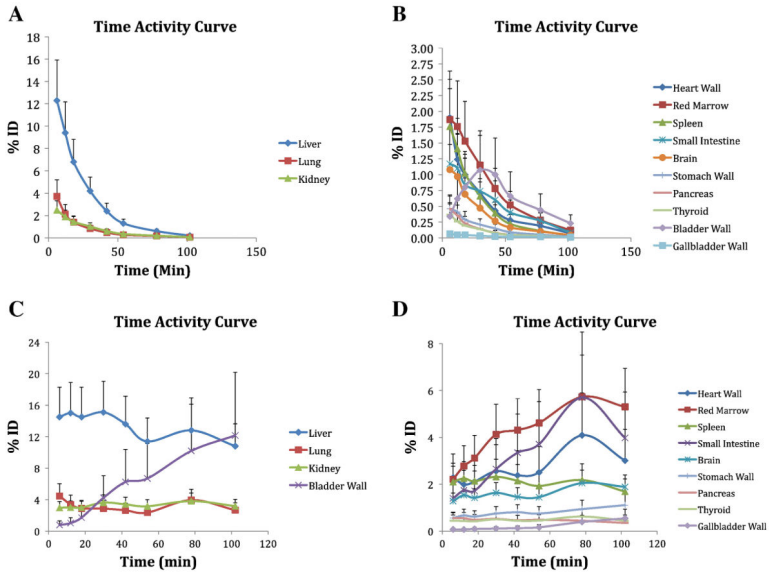

Figure 3.

Mean percentage injected dose (ID) as a function of time of the main organs. Vertical bars represent SD. Panels A and B show non-decay-corrected data for organs with higher (liver, lung, and kidney) and lower percentages of ID, respectively. Panels C and D show decay-corrected data for organs with higher and lower percentages of ID, respectively

TABLE 1

Organ Absorbed Doses for [11C]DAA1106

Organ	Absorbed Dose (μGy/MBq)
Adrenals	2.93 ± 0.50
Brain	2.39 ± 1.10
Breasts	1.00 ± 0.16
Gallbladder Wall	8.25 ± 4.29
Heart Wall	17.87 ± 5.25
Kidneys	11.25 ± 2.72
Liver	16.95 ± 4.61
Lower Large Intestine Wall	1.68 ± 0.24
Lungs	6.94 ± 2.75
Muscle	3.59 ± 0.27
Osteogenic Cells	2.68 ± 0.58
Ovaries	2.03 ± 0.34
Pancreas	10.66 ± 5.38
Red Marrow	3.67 ± 0.44
Skin	0.79 ± 0.04
Small Intestine	9.21 ± 4.22
Spleen	18.16 ± 12.00
Stomach Wall	6.67 ± 2.46
Testes	0.92 ± 0.09
Thymus	1.74 ± 0.24
Thyroid	3.81 ± 1.76
Upper Large Intestine Wall	2.53 ± 0.62
Urinary Bladder Wall	5.02 ± 2.52
Uterus	1.98 ± 0.32
Total Body	2.97 ± 0.25
Effective Dose (μSv/MBq)	4.06 ± 0.58
Effective Dose Equivalent (μSv/MBq)	5.89 ± 0.83

Values are mean ± SD for 10 male and 2 female participants. The dose for ovaries shown here is based on all participants, while that of testes is based on male participants only.